J Mater Sci: Mater Electron (2007) 18:721–728
DOI 10.1007/s10854-006-9101-8

Infrared absorption spectra of defects in carbon doped neutron-irradiated Si

C. A. Londos · G. D. Antonaras · M. S. Potsidi · D. N. Aliprantis · A. Misiuk

Received: 24 August 2006 / Accepted: 11 December 2006 / Published online: 5 January 2007
© Springer Science+Business Media, LLC 2007

Abstract Experimental data of infrared (IR) absorption measurements carried out on fast neutron irradiated carbon rich Cz–Si crystals were studied. Data from similar crystals, subjected prior to irradiation to thermal treatments at 1000 °C [(HT)] and thermal treatments at 1000 °C under high hydrostatic pressure [(HTHP)] of 11Kbar, were also studied. The time duration of both treatments was 5 h. After the irradiation the intensities of most of the observed bands were always stronger in the pre-treated material. Transformation of the defects upon post-irradiation isochronal anneals was investigated. Two out of six IR bands of the C_iC_s defect in the neutral charge state, at 543.5 and 635 cm^{-1}, were detected at room temperature [(RT)]. It is argued that another two bands at 918 and 1006 cm^{-1} arising in the spectra upon annealing of the C_iC_s bands are associated with the same carbon-related structure giving rise to the Si-PT4 electron paramagnetic resonance (EPR) spectrum. A band at 533 cm^{-1} shows the same thermal evolution with a defect giving rise to the Si-P6 EPR spectrum attributed to a multi-interstitial cluster in silicon. Differences observed in the evolution curves of the $C_iC_s(Si_I)$ defect (987, 993 cm^{-1}) between the as-grown and the pre-treated samples are considered and discussed.

C. A. Londos (✉) · G. D. Antonaras ·
M. S. Potsidi · D. N. Aliprantis
Solid State Section, Physics Department, University of Athens, Panepistimiopolis Zografos, Athens 157 84, Greece
e-mail: hlontos@phys.uoa.gr

A. Misiuk
Institute of Electron Technology, Al. Lotnikow 32/46, 02-668 Warszawa, Poland

1 Introduction

Energetic bombardment of silicon crystals produces different kinds of point defects. Most of the produced vacancies (V's) and self-interstitials (Si_I's) re-combine and annihilate in the course of irradiation. Some of the vacancies re-combine to form [1] di-vacancies and multi-vacancy clusters and some of the self-interstitials combine to form [2–4] di-interstitials and multi-interstitials clusters. The remaining vacancies and self-interstitials diffuse away and are eventually trapped by various impurities, deliberately added or inadvertently present in the material, forming stable defects which are distributed in the bulk. The class of the vacancy (V) and V-related defects has been investigated extensively by the commonly used spectroscopic techniques such as electron paramagnetic resonance (EPR), infrared (IR) absorption, photoluminescence (PL), deep level transient spectroscopy (DLTS), etc, and the researchers backed up by the theory were able to study and understand most of the properties, the structures, and generally the identities of these defects. As to the class of the (Si_I's) and the Si_I-related defects the corresponding picture is still incomplete [4, 5]. Due to the fact that the silicon self-interstitial is mobile [5] even at cryogenic temperatures, it was not possible to isolate and study this defect. Researchers turned instead to the study of the Si_I-related complexes, which are stable, in the hope that by understanding these larger defects, they will be able to gain some insight on the elusive nature of the Si_I. Thus, a number of multi-interstitial related centers as for example the $(Si_I)_2$, the $(Si_I)_3$ and the $(Si_I)_4$ clusters have been identified [2, 4, 6].

On the other hand, Si_I's form complexes with many impurities present in the lattice, as for example oxygen and carbon. It is well known that carbon [7, 8] is an efficient trap for Si_I's incorporating them in small defects. This ability of carbon and carbon-related defects to trap Si_I's has important technological impact, since they can reduce the formation of large interstitial clusters, as the [113] rod-like defects. Upon annealing, these [113] defects release Si_I's which affect the diffusion of dopant impurities, as for example boron and phosphorous in Si. Thus, they result [9] in transient enhanced diffusion (TED) which leads to detrimental effects in the electrically active region of the semiconductor devices.

C_i, C_iC_s and C_iO_i are the three main carbon-related defects produced in carbon-rich Czochralski grown (Cz–Si) material subjected to any kind of particle irradiation. For high irradiation doses, the above defects act as nucleation sites of the aggregation of Si_I's and complexes such as the $C_i(Si_I)$, $C_iC_s(Si_I)$ and $C_iO_i(Si_I)$ form [7, 10]. Apparently, the more we understand all these carbon-related defects the better we shall control and improve the yield and properties of the electronic devices.

It is well-known [11] that the degree of damage caused by neutron irradiation is much greater than that of electron irradiation and the number of primary defects is much larger in the first case. In addition, a special separation [12] of vacancies and self-interstitials is established reducing their annihilation. As a result, more Si_I's are available, facilitating the formation of larger concentration of (Si_I)-complexes. C-related complexes, where Si_I's participate directly or indirectly in their formation, also form in larger concentrations.

During processing of Si material thermal treatments are performed at various temperature ranges. An important temperature range, is that around 1000 °C, where diffusion of impurities and oxidation occurs. It will be interesting therefore to know the effect of thermal anneals at this temperature on the properties and behaviour of irradiation-induced defects. The application of high hydrostatic pressure during thermal treatments has also been used [13] as an additional means to investigate defect properties. Such treatments potentially offer significant gains in understanding and controlling defects in semiconductors.

The present paper is focused on the study of carbon-related defects and self-interstitial clusters in neutron irradiated Si, subjected to high temperature (HT) or high temperature - high pressure (HTHP) treatments prior to irradiation.

2 Experimental details

Three groups of samples purchased from MEMC, of 2 mm thickness, with initial concentrations $[O_i]_o = 7.2 \times 10^{17}$ and $[C_s]_o = 1.5 \times 10^{17}$ cm^{-3} were used in this study. The samples were irradiated with 5 MeV fast neutrons at a fluence of 1×10^{17} n cm^{-2}. Group I samples, (to be called hereafter M_1) were not subjected to any treatment prior to irradiation. Group II samples (to be called hereafter M_2) were subjected prior to irradiation to thermal treatment (HT) at 1000 °C, for 5 h and group III samples (to be called hereafter M_3) were subjected to thermal treatment at 1000°C under the application of high hydrostatic pressure (HTHP) of 11Kbar, for 5 h. The HT, HTHP treatments were carried out [14] in pure Argon atmosphere. After the irradiation 20 min isochronal anneals, of ~10°C steps, were performed in open furnaces. At the end of each annealing stage, infrared spectroscopy measurements were carried out, at room temperature, with a Jasco-IR 700 spectrometer of dispersive kind. The spectral resolution of the IR measurements was 1 cm^{-1}. The two-phonon absorption was always subtracted by using a reference sample of float-zone material. As we shall see below, the two-phonon absorption was not removed completely and the 604 cm^{-1} line due to substitutional carbon was perturbed. Taking this into account, the concentration of the C_s was determined from the strength of the 604 cm^{-1} LVM band, measured at room temperature, as follows. We followed the ASTM [15] procedure in conjunction with a conversion factor [16] 1×10^{17} cm^{-2}. It is known [17] that the 604 cm^{-1} peak is superposed on the strong intrinsic two-phonon band of silicon, actually located [18] on the shoulder of an intense lattice band at 610 cm^{-1}. In our samples, where the concentration of carbon is high, we drew in the spectra a straight baseline from 595 to 610 cm^{-1} and from the amplitude of the peak we calculated the concentration of substitutional carbon, in accordance with the above procedure. Comparisons of the given values of the $[C_s]$ in the untreated samples with the corresponding values calculated from our IR measurements allow us to estimate an error of about 5% in the determined values of $[C_s]$.

3 Experimental results

The values of the carbon concentration of all the samples after the various processes are presented in Table 1. In addition, Fig. 1 shows the evolution of the intensity of the 604 cm^{-1} peak (Fig. 2) of the substitutional carbon

Table 1 [C_s] of the samples after the various processes

Errors in the [C_s] were estimated about 5%

A	B	C	D	E
Sample	[C_s] × 10^{17} cm^{-3} initial	[C_s] × 10^{17} cm^{-3} after treatment	[C_s] × 10^{17} cm^{-3} after irradiation	Δ[C_s] × 10^{17} cm^{-3}
M_1(as grown)	1.52	1.52	0.49	1.03
M_2 (HT)	1.52	1.49	0.65	0.84
M_3 (HT-HP)	1.52	1.48	0.78	0.70

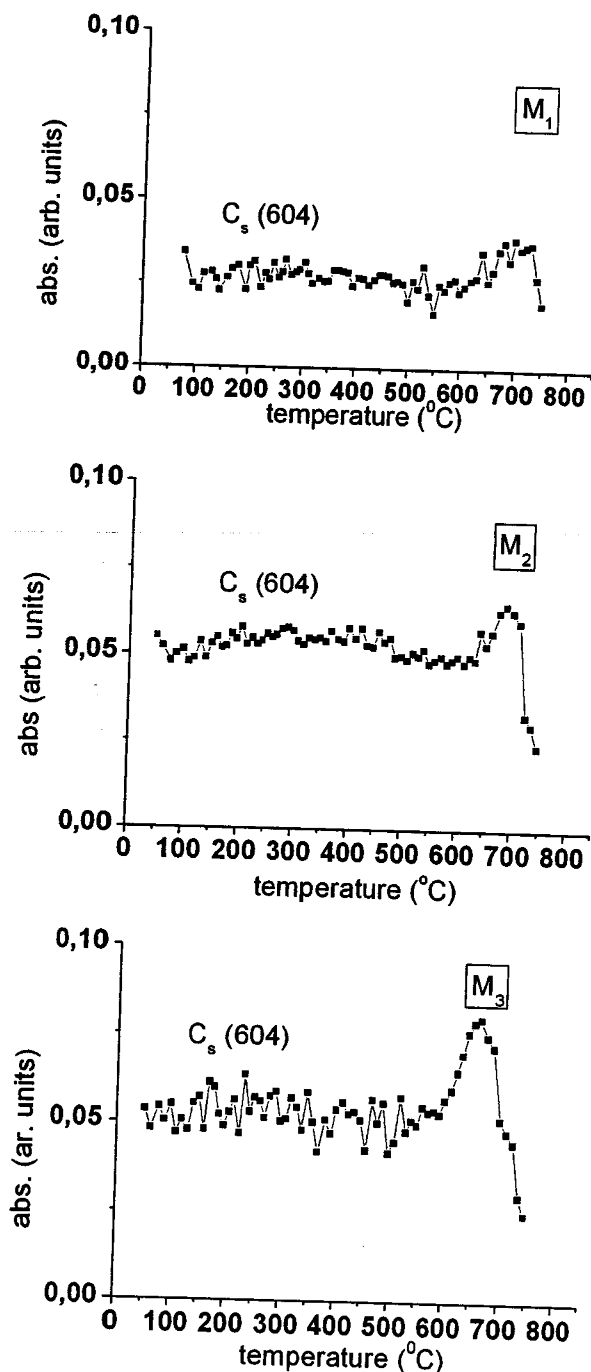

Fig. 1 The thermal evolution of the C_s (604 cm^{-1}) band

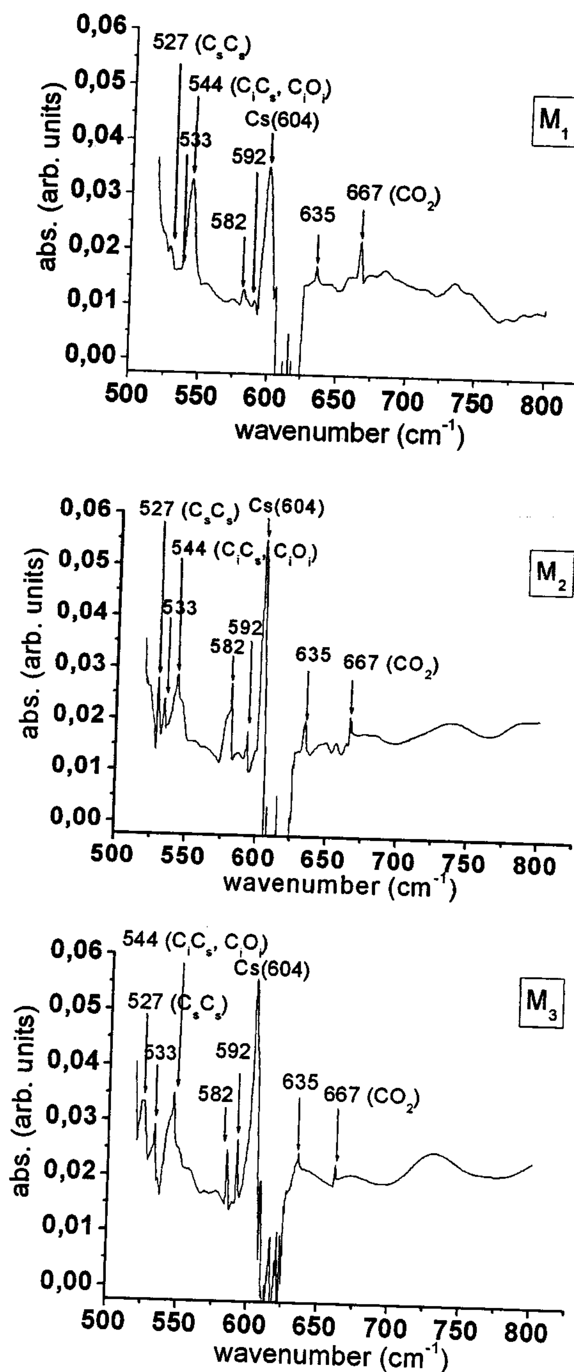

Fig. 2 Section of the absorption spectra (range 500–800 cm^{-1}) of the samples, after irradiation (at T = 77 °C)

after the irradiation. As it is immediately seen from this figure, the $[C_s]$ is larger in the samples subjected to HT and HTHP pre-treatments. At first we notice that IR spectroscopy measures the concentration of carbon at substitutional sites and not its total concentration in the material. It is well-known that C_sO_i complexes exist [7] in the material. These centers dissociate upon the treatments and the liberated carbon atoms are introduced into the Si matrix. Additionally, as a result of the treatments oxygen precipitates form, in the formation process of which carbon atoms participate [19–23] directly or indirectly in multiple ways: C_s atoms diffuse to regions adjacent to SiO_2 precipitates; carbon or carbon-related clusters, as for example C–O or C–Si_I complexes, act as nucleation sites for oxygen precipitates; coprecipitation of oxygen and carbon atoms occurs leading to the formation of SiO_2 and b-SiC precipitates, correspondingly. Thus, carbon atoms are removed from the Si lattice due to the precipitation process. Accordingly, the values of $[C_s]$ in column C of Table I reflect the effect of the above two contributions. Further on, as a result of the neutron irradiation, some precipitates are expected to be dissolved in the Si matrix releasing the containing carbon. A percentage of these carbon atoms restores at substitutional sites and this is reflected in the values of $[C_s]$ in column D, which are larger in the case of the pre-treated samples. Another percentage of these carbon atoms participates in the additional production of C-related centers. Thus, although the decrease in the $[C_s]$ after the irradiation is larger in the as-grown material, the intensity of the signals of the C-related defects is larger in the pre-treated material, as we shall see on the infrared spectra next. Thus, the seemingly controversial observation, that the radiation-induced bands in the IR spectra are always stronger in the pre-treated Si material although, as indicate the results presented in Table I, less carbon atoms were removed from substitutional positions as a result of the neutron irradiation, could be understood as follows: As we mentioned above besides the C_s atoms in the crystal, carbon atoms are also present in the form of C_sO_i complexes. Notice in addition, that carbon atoms may also be present [24] in unknown configurations, which are IR inactive and therefore undetectable in our measurements. The following picture emerges. In the initial stage of the heat treatments, carbon atoms trapped at these clusters are liberated and readily positioned at substitutional sites. As a result, the carbon content of the pre-treated material becomes substantially larger than the initial carbon concentration, $[C_s]_o = 1.52 \times 10^{17}$ cm^{-3}. In essence, the pre-treated samples have larger $[C_s]_o$ than the untreated one. At the later stages of the heat treatments a percentage of these carbon atoms either precipitates or is trapped in regions adjacent to oxygen precipitates. We assume that during neutron irradiation these precipitates liberate carbon atoms, which also participate in the formation of the carbon-related centers giving rise to IR bands in the spectra. This is an additional source of carbon atoms existing in the pre-treated material and contributing in the enhanced formation of C-related centers in the later material, making their corresponding bands stronger than those in the untreated sample. One should also take into account that in the pre-treated material, Si_I's liberated as a consequence of the precipitation process, are bound at the Si/SiO_2 interface. During irradiation, some of these Si_I's are released from the precipitate region and interact with C_s atoms transforming them to C_i, leading finally to an additional increase of the C-related defects.

Another point: we observe that the amplitude of the C_s band increases prior to decaying out. This phenomenon is common in silicon as already has been pointed out in the literature [25]. However, an adequate explanation is still lacking. In our case, this inverse annealing stage of the C_s band is more intense in the pre-treated samples.

Figure 2 shows a section of the IR spectra after the irradiation, for the samples M_1, M_2 and M_3. A number of peaks appear in the spectra. Some of them will be discussed below.

The 527 cm^{-1} peak has been previously studied [26, 27] and attributed to the C_sC_s defect. The 533 cm^{-1} peak appears as a faint signal in the IR spectra of the as-grown sample and has much stronger signals in the IR spectra of the pre-treated samples. Figure 3 shows the thermal evolution of this peak in the latter samples. The peak begins to disappear from the IR spectra around 170 °C, showing similar thermal stability with an EPR signal, Si-P6, attributed [3] to the di-interstitial center, although later studies [4] linked it with larger (Si_I)-complexes. We argue that the 533 cm^{-1} IR peak has the same origin as the Si-P6 EPR signal. Notice that the frequency value of the 533 cm^{-1} band lays in the range [4] where bands from multi-interstitial centers appear. A pair of bands at 530 and 550 cm^{-1} in neutron-irradiated Si also attributed [28] to (Si_I)-clusters disappear around 550°C, and apparently have different origin than our 533 cm^{-1} band.

The peak at 544 cm^{-1} has already been studied [29] in as-grown Si. It has been found that it is a complex band formed by the contribution of two bands at 543.5 and 545.5 cm^{-1} of the C_iC_s and C_iO_i defects, correspondingly. Figure 4(a) shows the deconvolution of the 544 cm^{-1} band, by using Lorentzian profiles, for the M_2

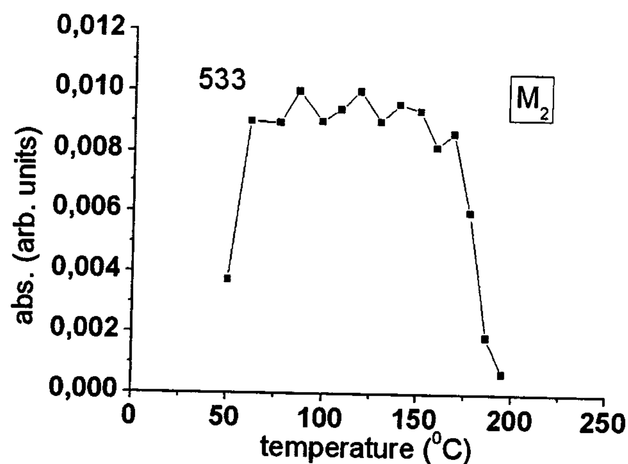

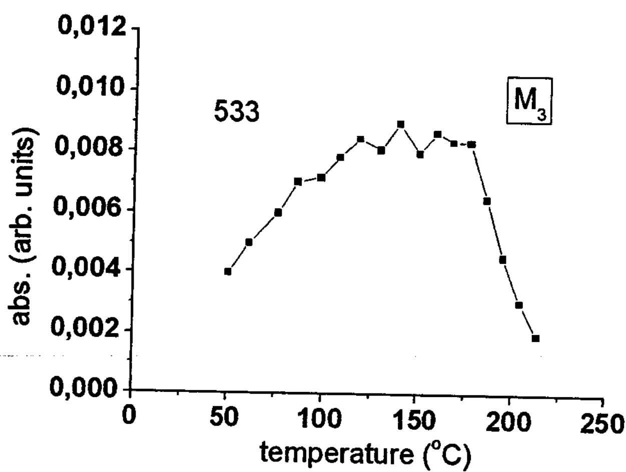

Fig. 3 The thermal evolution of the 533 cm^{-1} bands in the pre-treated samples

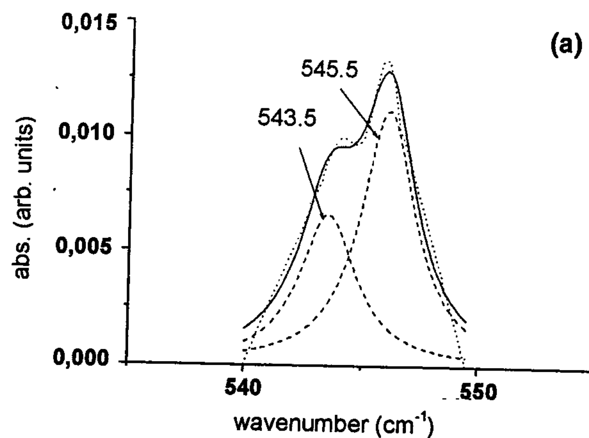

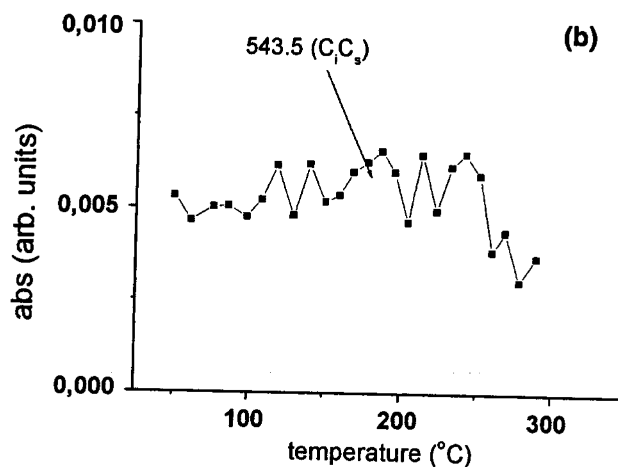

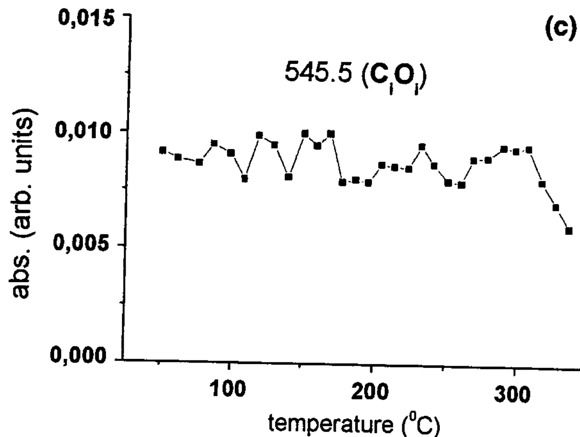

Fig. 4 (a) Deconvolution (Lorentzian profiles) of the 544 cm^{-1} band for the M_2 sample (b) the thermal evolution of the 543.5 cm^{-1} band and (c) the thermal evolution of the 545.5 cm^{-1} band

sample heat-treated at 1000°C, prior to irradiation. Figure 4(b) and (c) show the thermal evolution of the 543.5 and 545.5 cm^{-1} bands. The thermal evolution of these bands in the M_3 sample is quite the same. The larger intensities of the peaks in the M_2 sample enable us to detect in the spectra another peak at 635 cm^{-1} the thermal behavior of which (Fig. 5) is similar to that of the 543.5 cm^{-1} peak (Fig. 4(b)). Although the 635 cm^{-1} peak is present in the as-grown sample M_1 (Fig. 2) we failed to detect it in the previous study [27] due to the weakness of the signal. The 543.5 and 635 cm^{-1} bands are stable up to 250 °C. This is the temperature where the C_iC_s defect anneals out [7]. The later defect has [30] six bands in the B configuration, at 540.4, 543.3, 529.8, 640.6, 730.4 and 842.4 cm^{-1}. These values were reported for IR measurements taken at cryogenic temperature. Based on the thermal stability of the 543.5 and 635 cm^{-1} bands and their frequency values we attribute them to the C_iC_s defect, in the B configuration. The combination of thermal pre-treatments and neutron irradiation made it possible to detect signals from defects which are very weak and otherwise pass undetected at RT measurements. Unfortunately, the other four peaks of the C_iC_s center were not detected in this work. It is possible that a more suitable combination of the temperature, the duration of the pre-treatments and the fluence of the

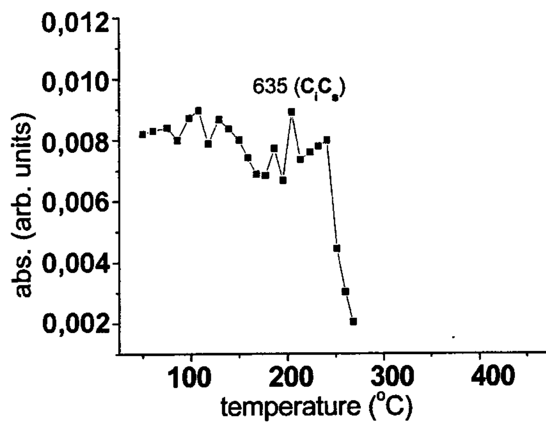

Fig. 5 The thermal evolution of the 635 cm^{-1} band for the M_2 sample

fast neutrons would enable us to detect them at room temperature.

Figure 6(a) shows another section of the absorption spectra in the range 800–1100 cm^{-1} for all samples. Besides the well-known peaks of VO (828 cm^{-1}) and C_iO_i (860 cm^{-1}) defects and the peaks of $C_i(Si_I)$ (953, 960 cm^{-1}), $C_iO_i(Si_I)$ (934, 1018 cm^{-1}) and $C_iC_s(Si_I)$ (987, 993 cm^{-1}) structures which have been already studied [7, 29], some other peaks appear in the spectra which will not be discussed in this work. Figure 6(b) shows the same range in the spectra as Fig. 6(a) after the isochronal anneal sequence at 304 °C, for all samples. The pair of peaks at 918, 1006 cm^{-1} emerge in the spectra as the two observed peaks at 543.5 and 635 cm^{-1} of the C_iC_s defect anneal out. (Fig. 7) depicts this phenomenon for the sample M_2. The picture is quite the same for the sample M_3.

The annealing out of the di-carbon center is a very complicated process, not completely understood. At least four processes occur [31, 32] during its anneal: i) break-up of the center and the emission of a C_i atom ii) multiple recapture of C_i atoms iii) motion of a diffusing species to the di-carbon center and iv) a growth process superimposed on the destruction of the center. Photoluminescence (PL) measurements has shown that a PL line at 953 meV (7686 cm^{-1}) grows when the G-line of the C_iC_s defect anneals. Electron Paramagnetic Resonance (EPR) measurements has shown that the anneal

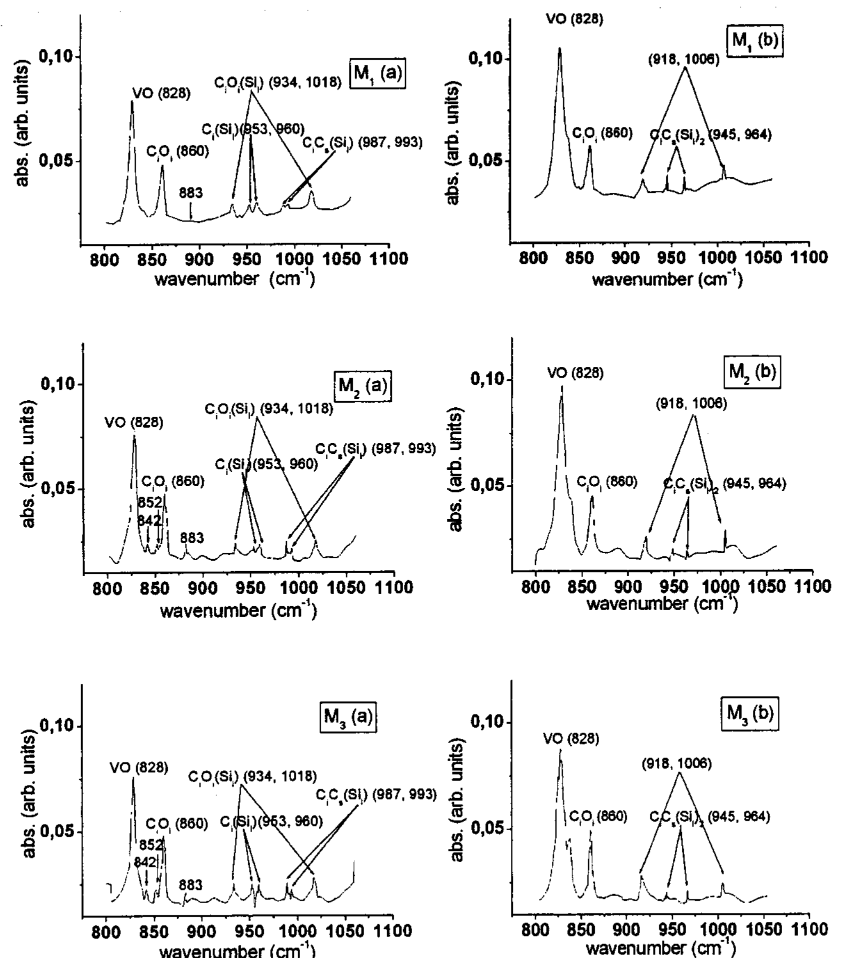

Fig. 6 Section of the absorption spectra (range 800–1100 cm^{-1}) (**a**) after irradiation (at T = 77°C), and (**b**) after isochronal anneal sequence (at T = 304°C) for all samples, correspondingly

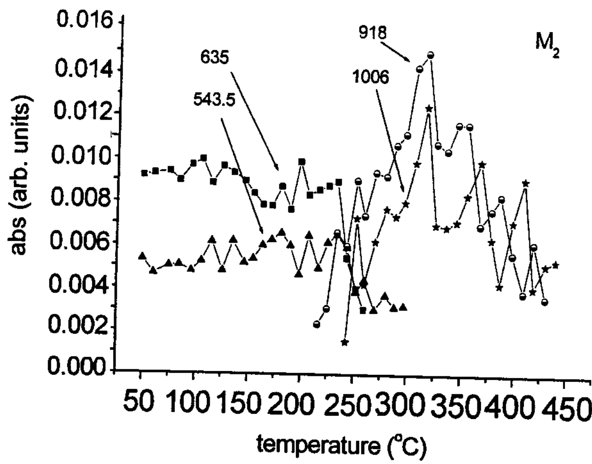

Fig. 7 The thermal evolution of the (543.5, 635 cm^{-1}) and the (918, 1006 cm^{-1}) pairs of bands in the M_2 sample

of a so-called Si-PT1 signal related to the $(C_s–Si_I–C_s)^0$ complex, is accompanied by the emergence of a Si-PT4 signal. It was suggested [33] that the latter signal is either a $(C_s–Si_I–C_s)^0$ complex slightly disturbed by the capture of additional Si or C atoms or it is an intermediate state of the $(C_s–Si_I–C_s)^0$ complex during annealing where a bond between two C_s atoms is formed and a Si_I atom is stabilized near the $C_s = C_s$ complex. The thermal evolution of our 918, 1006 cm^{-1} IR bands is quite similar to that of the Si-PT4 EPR signal. We correlate these bands with the Si-PT4 EPR signal. It is also possible that the 953 meV PL line has the same origin.

The pair of peaks at 945, 964 cm^{-1} arising in the spectra upon annealing out of the two bands at 987, 993 cm^{-1} have been studied recently [34] and correlated with the $C_iC_s(Si_I)_2$. Figure 8 shows the thermal evolution of the above peaks in all the samples. It is immediately observed that in the samples heat-treated at 1000 °C, prior to irradiation, the thermal evolution curves of the defects is somewhat different. Actually, the emergence of the (945 and 964 cm^{-1}) bands occurs earlier than the beginning of the decay of the (987 and 993 cm^{-1}) pairs. This could be explained as follows. In these samples, oxygen precipitates are expected to form [19]. Their formation is accompanied by the emission of self-interstitials. A large amount of them is trapped at the interface between the precipitate and the Si matrix. These regions of stored Si_I's are expected to act as additional sources for self-interstitials, during the isochronal anneal as the temperature increases. The temperature of their release depends on the particular parameters of the pre-treatments, that is the temperature of the thermal treatment, its time duration and the simultaneous application or not of high hydrostatic pressure. It possibly also depends on

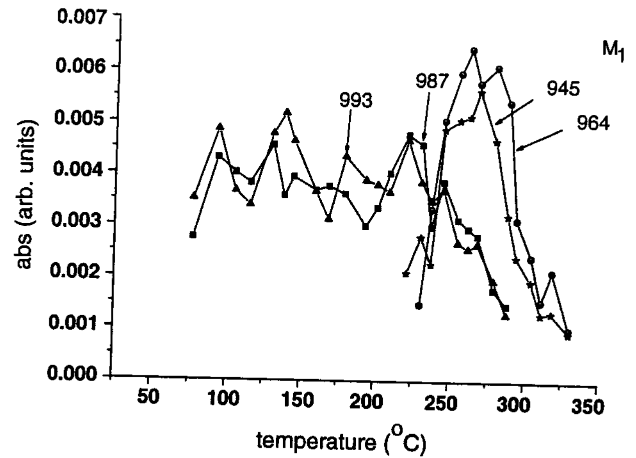

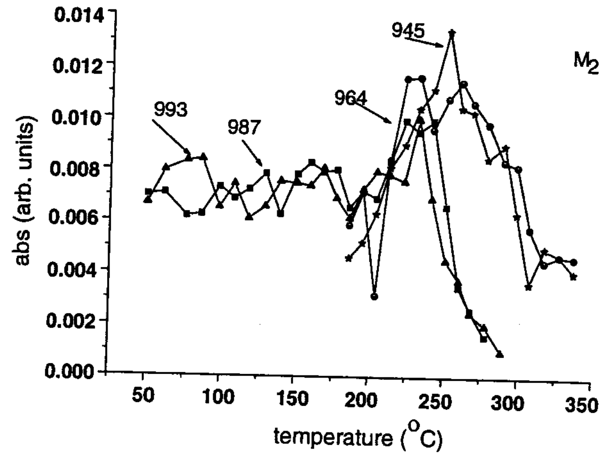

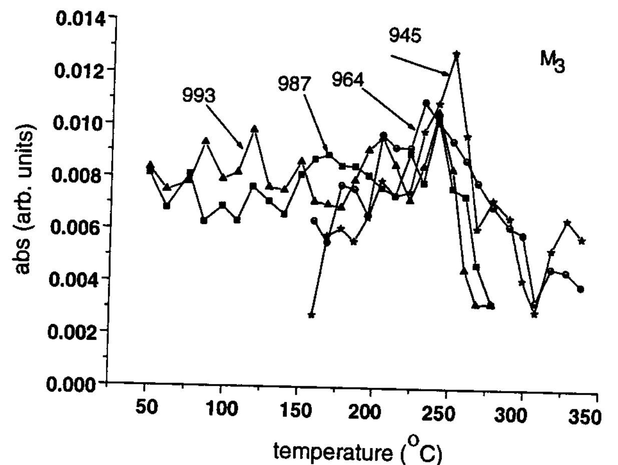

Fig. 8 The thermal evolution of the (987, 993 cm^{-1}) and the (945, 964 cm^{-1}) pairs of bands for all samples

and the kind of irradiation. We assume that in our case, during the isochronal anneal sequence, at temperatures ~180°C and higher, these regions begin to liberate Si_I's, which participate in the following reactions:

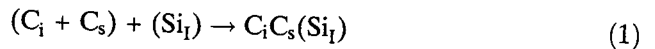

$$(C_i + C_s) + (Si_I) \rightarrow C_iC_s(Si_I) \quad (1)$$

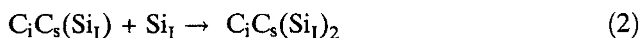

$$C_iC_s(Si_I) + Si_I \rightarrow C_iC_s(Si_I)_2 \quad (2)$$

In the temperature range 180–230 °C both reactions occur. Reaction (1) accounts for the increase of the (987, 993 cm^{-1}) signals due to the additional formation of $C_iC_s(Si_I)$ centers. Reaction (2) accounts for the appearance in the spectra of the (945–964 cm^{-1}) bands attributed [34] to the $C_iC_s(Si_I)_2$ complex. Above 230 °C, reaction (2) prevails leading to the transformation of all the existing $C_iC_s(Si_I)$ to the $C_iC_s(Si_I)_2$ defects.

Finally, it is worth noting that the behavior of the peaks of the samples pre-treated at 1000 °C with or without the application of hydrostatic pressure is quite similar. Besides small differences in their amplitudes, the applied pressure has not produced any significant changes in their behavior as it appears in our IR spectra. Although the sample M_3 is expected to contain a larger number of smaller precipitates and a more homogeneous distribution of them than in the sample M_2, the behavior of the defects is about the same in these two samples. It seems that the application of hydrostatic pressure at 1000 °C, due possibly to the short duration of the treatment (5 h), has not any significant influence on the thermal evolution of the radiation defects.

4 Conclusions

The combination of neutron irradiation and thermal pre-treatments enables us to observe weak signals from C-related and (Si_I)-related defects in carbon-rich Czochralski grown silicon. Thus, two bands of the C_iC_s defect in configuration B at 543.5 and 635 cm^{-1} were detected at room temperature. The anneal of these bands is accompanied by the growth in the spectra of two other bands at 918 and 1006 cm^{-1} exhibiting the same evolution with the Si-PT4 EPR signal previously attributed to a perturbed geometry of the $(C_s–Si_I–C_s)^o$ defect. A band at 533 cm^{-1} is suggested to be correlated with the same multi-interstitial center giving rise to the Si-P6 EPR signal.

References

1. Y.-H. Lee, J.W. Corbett, Phys. Rev. **B9**, 4351 (1974)
2. Y.-H. Lee, N.N. Gerasimenko, J.W. Corbett, Phys. Rev. **B14**, 4506 (1976)
3. Y.-H. Lee, Appl. Phys. Lett. **73**, 1119 (1998)
4. A. Carvalho, R. Jones, J. Continho and P.R. Briddon, Phys. Rev. **B72**, 155208 (2005)
5. G.D. Watkins, Mater. Sci. Semicond. Process. **3**, 227 (2000)
6. S. Hayama, G. Davies, K.M. Itoh, J. Appl. Phys. **96**, 1754 (2004)
7. G. Davies, R.C. Newman, in *Handbook on Semiconductors*, vol. 3b. ed. by S. Mahajan (Elsevier Science B.V., Amsterdam) (1996), p. 1557
8. S. Nishikawa, A. Tanaka, T. Yamajl, Appl. Phys. Lett. **60**, 2270 (1992)
9. M. Kohyama, S. Takeda, Phys. Rev. **B46**, 12305 (1992)
10. G. Davies, Mater. Sci. Forum. **38–41**, 151 (1989)
11. K. Laithwaite, R.C. Newman, D.H.J. Totterdell, J. Phys. C. **8**, 236 (1975)
12. N. Fukata, T. Ohori, M. Suezawa, H. Takahashi, J. Appl. Phys. **91**, 5891 (2002)
13. A. Misiuk, in *Frontiers of High Pressure Research II, Application of High Pressure to Low-Dimensional Electronic Materials*, Series II-vol.48. ed. by H.D. Hochheimer, B. Kuchta, P.K. Dorhout, J.L. Yarger (Kluwer Academic Publishers, Dordrecht, 2001), p. 275
14. A. Misiuk, Mater. Phys. Mech. **1**, 119 (2000)
15. ASTM standard test method F123–86
16. J.L. Regolini, J.P. Stroquert, C. Ganter, P. Siffert, J. Electroch. Soc. **133**, 2165 (1986)
17. F.A. Johnson, Proc. Phys. Soc. London **73**, 265 (1959)
18. F.L. Vook, H.J. Stein, Appl. Phys. Lett. **13**, 343 (1965)
19. A. Borghesi, B. Pivac, A. Sassella, A. Stella, J. Appl. Phys. **77**, 4169 (1995)
20. H. Bender, Vanhellemont, in *Handbook on Semiconductors*, vol 3b (Elsevier Science B.V., Amsterdam, 1994), p. 1637
21. G.S. Oehrlein, J.L. Lindstrom, J.W. Corbett, Appl. Phys. Lett. **40**, 241 (1982)
22. U. Gosele, Mater. Res. Soc. **59**, 419 (1986)
23. F. Simura, T. Higuchi, R.S. Hockett, Appl. Phys. Lett. **53**, 69 (1988)
24. R.C Newman, Mater. Res. Soc. **59**, 403 (1986)
25. G. Davies, E.C. Lightowlers, M. Stavola, K. Bergman, B. Svenson, (1987) Phys. Rev. **B35**, 2755
26. E.V. Lavrov, B. B. Nielsen, J.R. Byderg, B. Hourasine, R. Jones, S. Oberg., P.R. Briddon, Phys. Rev. **B62**, 158 (2002)
27. C.A. Londos, M.S. Potsidi, E. Stakakis, Physica. **B340–342**, 551 (2003)
28. R.C. Newman, D.H.J. Totterdell, J. Phys. **C8**, 3944 (1975)
29. C.A. Londos, M.S. Potsidi, G.D. Antonaras, A. Andrianakis, Physica. **B376–377**, 551 (2006)
30. V. Lavrov, L. Hoffman, B. Bech Nielsen, Phys. Rev. **B60**, 8081 (1999)
31. G. Davies, K.T. Kun, T. Reade, Phys. Rev. **B44**, 12146 (1991)
32. T. K. Kwok, Phys. Rev. **B51**, 17–188 (1995)
33. R. Laiho, M.P. Vlasenko, L.S. Vlasenko, Solid State Commun. **124**, 403 (2002)
34. M.S. Potsidi, C.A. Londos, J. Appl. Phys, **100**, 033523 (2006)